The Study of the Clinical Dose Distribution for Dynamic Virtual Wedge Algorithm

Jao-Perng Lin[1,2,3], Tung-Hao Chang[1,4], Ai-Yih Wang[2], Mu-Tai Liu[1,2,3,5], Yuan-Rong Chen[1,4], Chiung-Wen Kuo[2], Yuan-Chun Lai[1]

Background and purpose: This study describes our experience in clinical application of the virtual wedge (VW), including VW angles verification, wedge factors, percentage depth doses and profiles.

Methods: We used a Wellhöfer IC15 0.13cm^3 ion chamber, a CU500E 6177 electrometer, and a 48 × 48 × 40 cm^3 water phantom. An ion chamber array detector (CA24, Wellhöfer Dosimetrie) was employed to measure the profiles. Simultaneously controlling the movement of one of the upper collimator jaws and varying the dose rate during irradiation created the virtual wedge. This procedure produced a dose profile comparable to that achieved from a physical wedge (PW).

Results: The measured wedge angles were consistent with the machine setup angles to within 1°. All wedge factors of the VW were equal to 1.0 within 1%, except for 60° wedges for 20×20 to 24×24 cm^2 field sizes where they deviated by 2-3%. The percentage depth doses (PDD) of VW were closer to those of an open field.

Conclusion: VWs are more flexible than PWs, and they have practical and dosimetric advantages. VWs are more convenient for treatment setup, and they have various arbitrary angles. VWs are a positive replacement for PWs. (*Changhua J Med* 2003;**8**:87-97)

Key words: virtual wedge, wedge factor, virtual wedge angle

Introduction

Wedge-shaped isodose distributions have important roles in clinical radiotherapy. They are used to optimize treatment in conditions such as sloped patient surfaces and irregularly shaped tumor volume. These distributions were developed using different methods. One common method was to place a lead attenuator, or a physical wedge (PW), in the x-ray beam path. Although this approach has several limitations, PWs are simple to implement in clinical practice. However, they are limited to field size and available wedge angles. Often only four types are typically available. As a result, of the high density and atomic number of the materials used for physical wedges, they are heavy and create additional low energy electrons and photon scatters. Furthermore, treatment time is increased because of the diminished primary beam intensity and time required for installation and removal.

With the development of computer control technique, collimator jaws can be moved during irradiation, which permits the virtual simulation of PW profile possible. Notably, Kijewski et al. first proposed this concept [1]. This technique does not require handling of PWs, which therefore facilitates accurate and faster treatment. Subsequently, dynamic wedge (DW) [2,3] and virtual wedge (VW) [4,5] were proposed. They are both computer-controlled modalities that generate wedge-shaped profiles through the synchronization of dynamic jaw motion with dose output.

However, VW differs from DW in two major aspects. First, during treatment, the moving jaw closes and then fully opens, as the dose is delivered. Second, the jaw moves at a constant speed while the dose rate is modified as a function of time. The dose rate is varied according to the following equations [5]:

$$MU(x) = MU(0)\exp(-\mu x \tan\theta) \quad (1)$$

$$\frac{dMU}{dt} = vMU(0)\mu \tan\theta \exp(-\mu x \tan\theta) \quad (2)$$

[1]Department of Radiation Oncology, Changhua Christian Hospital, Changhua, Taiwan, [2]Department of Radiological Technology, Yuan-Pei Institute of Science and Technology, Hsinchu, Taiwan, [3]Department of Oncology, National Taiwan University Hospital, Taipei, Taiwan, [4]Department of Nuclear Science, National Tsing Hua University, Hsinchu, Taiwan, [5]Department of Medicine, Chung Shan Medical University, Taichung, Taiwan

Received: September 23, 2002 Revised: January 14, 2003 Accepted: February 18, 2003

Reprint requests and corresponding to: Dr. Tung-Hao Chang, Department of Radiation Oncology, Changhua Christian Hospital, 135 Nanhsiao Street, Changhua 500, Taiwan.

where MU(x) is the number of monitor unit (MU) that is given while a point at position x is irradiated. Then, MU(0) is the number of MU at $x = 0$ and is also the number of MUs that were entered at the machine console. As well, θ is the desired wedge angle, v is the speed of moving jaw and μ is the effective attenuation coefficient of the beam.

VW has advantages over PW. VW eliminates the potential hazard to patients of a dropped wedge, and VW has a wide and continuously variable wedge angle, typically from 15 to 60 degrees.

In this study, the data required prior to clinical application of the VW, including VW angles verification, wedge factors, percentage depth doses and profiles, are described. In addition, clinical cases that used the VW wedge technique in their treatment plans are presented. Finally, several relevant changes in comparison to PWs are presented.

Materials and Methods

We used a dual energy (6 and 15MV photons) Siemens PRIMUS3008 linear accelerator that has both the PW and VW, which moves dynamically through two upper jaws during treatment. Accelerator control software that was designed according to Equation (2) provided the coordinated movement of an upper jaw and varying output to create wedge-shaped profiles. In order to use VW in the clinic, wedge angles, wedge factors (WFs), percentage depth doses (PDDs) and profiles were measured using a 0.13 cm^3 ion chamber (IC15, Wellhöfer Dosimetrie) and an electrometer (CU500E 6177) in a 48 × 48 × 40 cm^3 water phantom. An ion chamber array detector (CA24, Wellhöfer Dosimetrie) was used to measure the profiles.

Virtual wedge angles

Effective attenuation coefficient in Equations (1) and (2) varies as a function of energy. A default effective attenuation coefficient, μ_{def}, was required for each energy when implementing VW. A calibration factor, c, was used to adjust effective attenuation coefficient. Accordingly, μ_{def} was multiplied by c factor and produced $\mu = c \times \mu_{def}$. Furthermore, by adjusting the c factor, the VW angle was modified to achieve calibration.

According to Siemens acceptance test procedure, measurement of only four points were required to determine the wedge angle. These points consist of two points along a beam profile taken at 10 cm depth and two central axis points taken at 9 and 11 cm depths. After measuring the four points, the wedge angle was calculated as follows:

$$wedge\ angle = \tan^{-1}\left(\frac{|D_p - D_q|/\Delta d}{|D_9 - D_{11}|/2}\right) \quad (3)$$

where D_p and D_q are integrated doses at points p and q, respectively. Points p and q are the off-axis point at 10 cm depth. The values are F/4 cm for 15 and 30° wedge angles and F/6 cm for 45 and 60° ones. F is the field size. D_9 and D_{11} are integrated doses at 9 and 11 cm depth on the central axis, respectively.

To determine the wedge angle for the specified field size and Equation (3), profiles were measured for 15°, 30°, 45°, and 60° wedge angles for 20 × 20 cm^2 field size at the source to surface distance (SSD) of 90 cm. The calculated wedge angles were compared with the machine setup angles.

Wedge factors

According to Equation (1), the output factors of the VW at the central axis were identical to those of the open field in the same field size. This is because the MUs delivered at the position are identical. Moreover, the WF is the dose ratio of the wedge field to the corresponding open field. Therefore, in theory, WF of VW will be close to unity within all field sizes.

To verify this, the relationship of WF, which is dependent on energy, wedge angle and field setting in the wedge direction was determined. Field sizes varied from 4 × 4 to 25 × 25 cm^2. The reference point at the central axis was SSD 100 cm and had a 5 cm and 10 cm depth for 6 MV and 15 MV, respectively. The data were measured with both the VW and the PW.

In order to observe the WF increments within various field sizes, all measurements were normalized to the reference field size of 10 × 10 cm^2. At a given depth, d, the WFs for various field sizes, A, were compared to that determined for the reference field size. A field size-normalized relative wedge factor (RWF_A) for various field sizes, A, was defined as

$$RWF_A = WF(d, A) / WF(d, 10\times10) \quad (4)$$

where RWF_A provides a direct measure of the field size that is dependent of the WF at a given depth to that determined for a 10 × 10 cm^2 field size.

Percentage depth doses

The water phantom and ionization chamber were used to measure the open, virtual and physical wedge PDDs. The field sizes were 5 × 5, 10 × 10 and 20 × 20 cm^2. However, to measure the PDD at various depths,

the ion chamber used for VW was in "gradient dependent" scan mode, not "continuous scan mode" for both the open and PW.

Profiles

To measure profiles and dose of the VWs or DWs, a dosimeter must remain static. Point measurement from an ion chamber provides the most accurate dose distribution. However, this procedure is very time-consuming because the dose at each measurement point must be obtained by integrating dose during the entire exposure.

A CA24 ion chamber array detector and a water phantom were used to obtain wedge profiles. Dose profile measurements for nonphysical wedges with the CA24 ion chamber array detector have been reported [6]. The chamber array detector has 23 ion chambers that are spaced 2.0 cm apart in a linear fashion. It also has an additional reference chamber that Wellhöfer control software (WP700) and hardware propels, and can be moved precisely in three dimensions in the water phantom. Profiles are measured along the chamber array axis, *i.e.* the axis along which all the chambers are aligned. Shifting the entire chamber array to a specific spacing produces spatial resolution that is finer than the 2.0 cm chamber-to-chamber distance along this direction. Data presented herein were measured with a spacing of 5 mm.

Profiles were measured at the depth of maximum dose (d_{max}), 5, 10, and 20 cm depths in both VWs and PWs using the chamber array for 20 × 20 cm^2 field at wedge angles of 15° to 60°. All profiles were normalized to the measured central-axis value at d_{max}. Compare profiles with VW and PW.

Treatment plan

Except TMS (Helax AB, Sewden) and Pinnacle^3 (ADAC, CA), most treatment planning systems model VW identically to PW. Therefore, a treatment planning system may not be equipped to model an arbitrary wedge angle. In this study, Pinnacle^3 was used and the modeling of the wedged beam profiles can assume various forms with VW, which are independent of PW.

To use VW clinically, the Pinnacle^3 treatment planning system was applied. During VW implementation, default parameters were provided, which could be defined during the radiotherapy treatment planning system commissioning process of VW. These include machine type, wedge orientation, jaw speed, jaw ranges, beam energy, effective linear attenuation coefficient (μ), c factor, dose rate ranges as well as any desired WFs. The Convolution/Superposition algorithm was used to calculate three-dimensional dose distributions with a 0.25 cm resolution. Common axes and scales superimposed both the calculated and measured profiles, which were compared.

Clinical treatment plans (physical versus virtual wedges) were compared for a larynx cancer patient. The plan had four fields with directions of 45°, 90°, 270°, and 315°, respectively. The relative beam weighting was 3: 2: 2: 3 to the four beams, respectively. In addition, 30° wedges were used for the 45° and 315° beams. An additional VW plan was applied to the same patient and 40° VW was used.

Results

Virtual wedge angles

After adjusting the c factors, the measured wedge angles were consistent with the machine setup angles with an error within 1°, except for 6 MV and 15 MV, which were 30 and 15 wedge degrees, respectively (Table 1).

Table 1. Comparison of wedge angles between machine setup and the calculated values.

	6 MV		15 MV	
Machine setup angle (deg)	Calculated value(deg)	Deviation (deg)	Calculated value(deg)	Deviation (deg)
15	14.27	-0.73	13.68	-1.32
30	31.19	+1.19	29.14	-0.86
45	45.57	+0.57	45.60	+0.60
60	59.85	-0.15	60.45	+0.45

Virtual wedge factors

All WFs of VW were equal to 1.0 with an error within 1%, except for 60° wedges at 20 × 20 to 24 × 24 cm^2 field sizes where they deviated by 2-3%. The experimental results indicated that WFs of VW would influence large wedge angles and field sizes in MU calculations. The WFs of VW have a slight dependence on field size. While the wedge factor variation with various field sizes was small (0.2-2.8%) for VW, it was larger (0.9-4.6%) for PW (Figure 1). The increment of WFs of VW may be due to the increase in scattering that occurs as the fields expand during the moving process, or the VW treatments may require more MUs for the large field with large wedge angles.

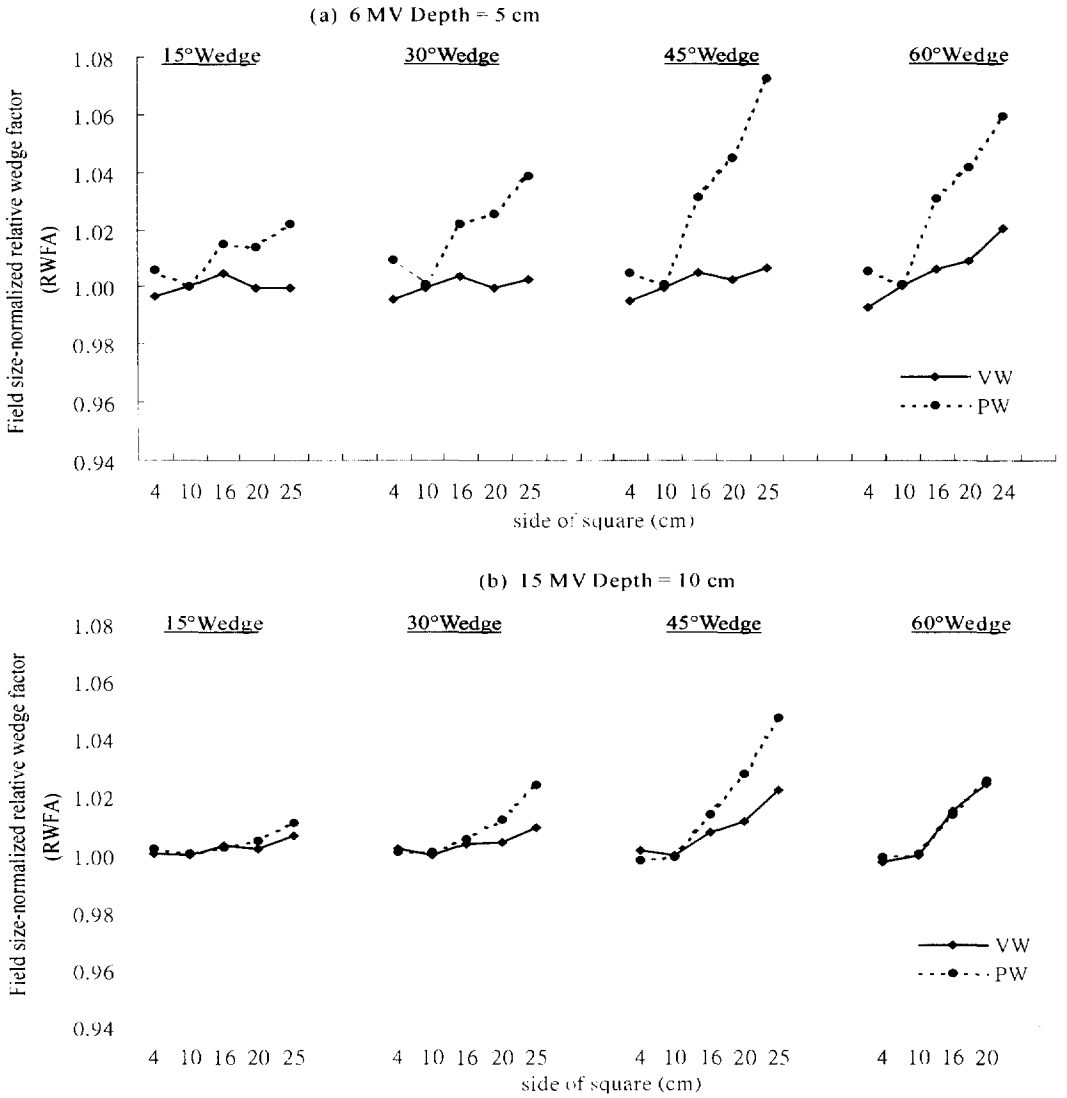

Figure 1. Field size-normalized relative wedge factor (RWF_A) at 5 and 10 cm depths as a function of field size for (a) 6 and (b) 15 MV photon beams, respectively.

Figure 1 compares the RWF_A of 4 × 4, 10 × 10, 16 × 16, 20 × 20, 25 × 25 cm^2 field sizes at 5 cm (for 6 MV) and 10 cm (for 15 MV) depths for VWs with those of PWs. RWF_A increases generally as field size increases. However, with various field sizes and wedge angles, the RWF_A increments for VW were smaller than PW. The field size dependence of WFs for PW may be due to back-scattered radiation from wedge filter as well as the head scatter radiation [7]. Moreover, those for VW are probably due to transmission through the moving collimator jaw and extrafocal radiation under this jaw.

Percentage depth doses

Figure 2 presents the measured PDDs for 6 MV photons. The good agreement between open and VW fields on PDDs indicated that PDD measurements for large number of VW fields were not required. The differences (compared with the PDDs for the open fields) were consistently within 0.8%, for both wedge angles. Table 2 compares PDDs for 5 × 5 and 20 × 20 cm^2 field sizes and 60° wedge angle. For the PW, the differences of PDDs, as compared with those of the open field, were larger. This influences both MU calculations as well as conventional treatment planning.

Table 2. Percent depth dose (PDD) comparisons for open field, virtual wedge and physical wedge.

	6 MV				15 MV			
Field size (cm^2)	5×5		20×20		5×5		20×20	
Depth (cm)	5	20	5	20	5	20	5	20
Open (%)	85.3	35.5	88.6	43.5	94.4	47.8	93.5	52.4
Virtual wedge (%)	85.1	34.9	88.7	43.7	93.9	47.8	93.1	52.6
Physical wedge (%)	86.5	37.9	88.9	45.6	96.0	49.9	95.0	54.0

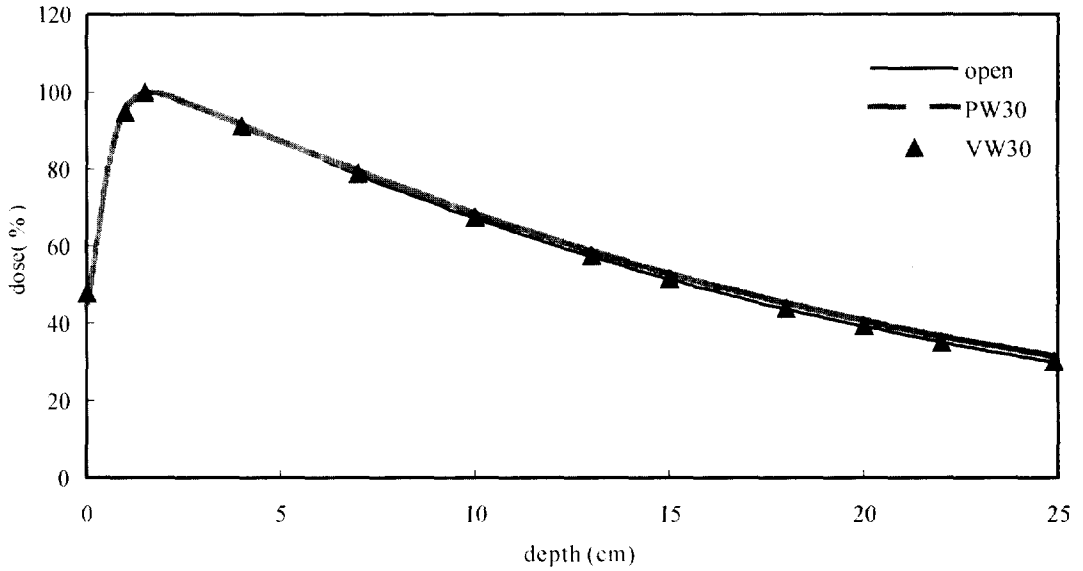

Figure 2. Depth doses for 6 MV open field ("open"), 30° virtual wedge ("VW30") and physical wedge ("PW30") of 10×10 cm^2.

Table 3. This table illustrate the dose of the 6 MV 20×20 cm^2 outside field for both 45° physical and virtual wedges.

Distance from field edge (cm)	The dose (cGy) outside the field 20 × 20 cm^2				
	Open	PW-heel	VW-heel	PW-toe	VW-toe
2	6.4	8.5	3.9	17.4	11.8
5	3.4	7.1	1.6	10.7	5.7
8	2.2	5.7	2.0	8.2	3.1
10	1.5	5.0	0.5	6.8	3.6

Profiles

Figures 3 and 4 illustrate the profile comparison of the four types of wedge angles in 20 × 20 cm^2 fields for both VWs and PWs. Dose was normalized to 100% at d_{max}, along the central axis. VWs and PWs were different, especially for 6 MV 45° wedge angle and 15 MV 60° wedge angle. Although both have similar profiles, they could not be exchangeable in the treatment planning system.

The other significant clinical parameter that was noted was dose reduction outside the field. Table 3 lists the experimental results of outside dose for both open and wedged fields both at the thick end ("heel") and the thin end ("toe"). The dose increase varies strongly with the wedge orientation, and the toe direction has a higher dose.

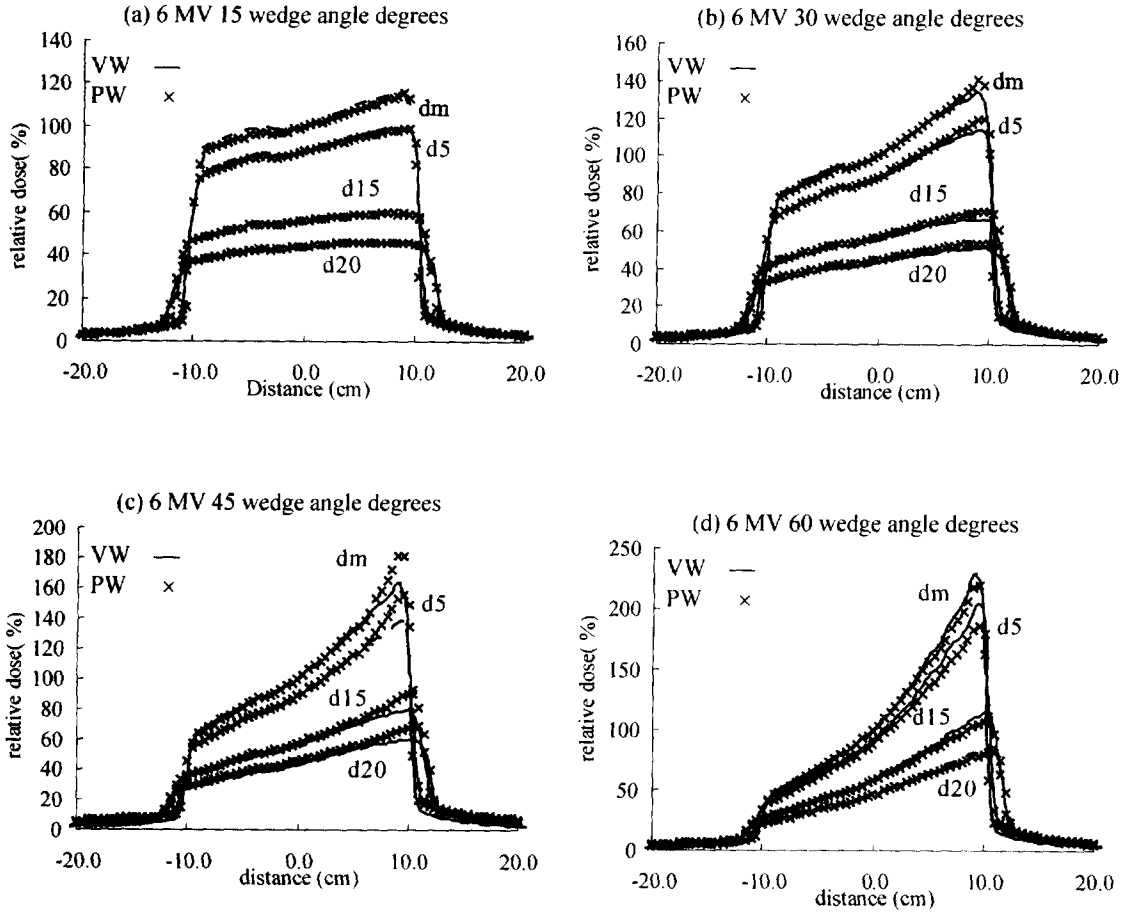

Figure 3. Profiles of the 6 MV 20×20 cm^2 field with physical wedges ("PW") and virtual wedges ("VW") at depths of d_{max} ("dm"), 5 cm ("d5"), 15 cm ("d15"), and 20 cm ("d20"). Dose is normalized to 100% at the d_{max} along the central axis.

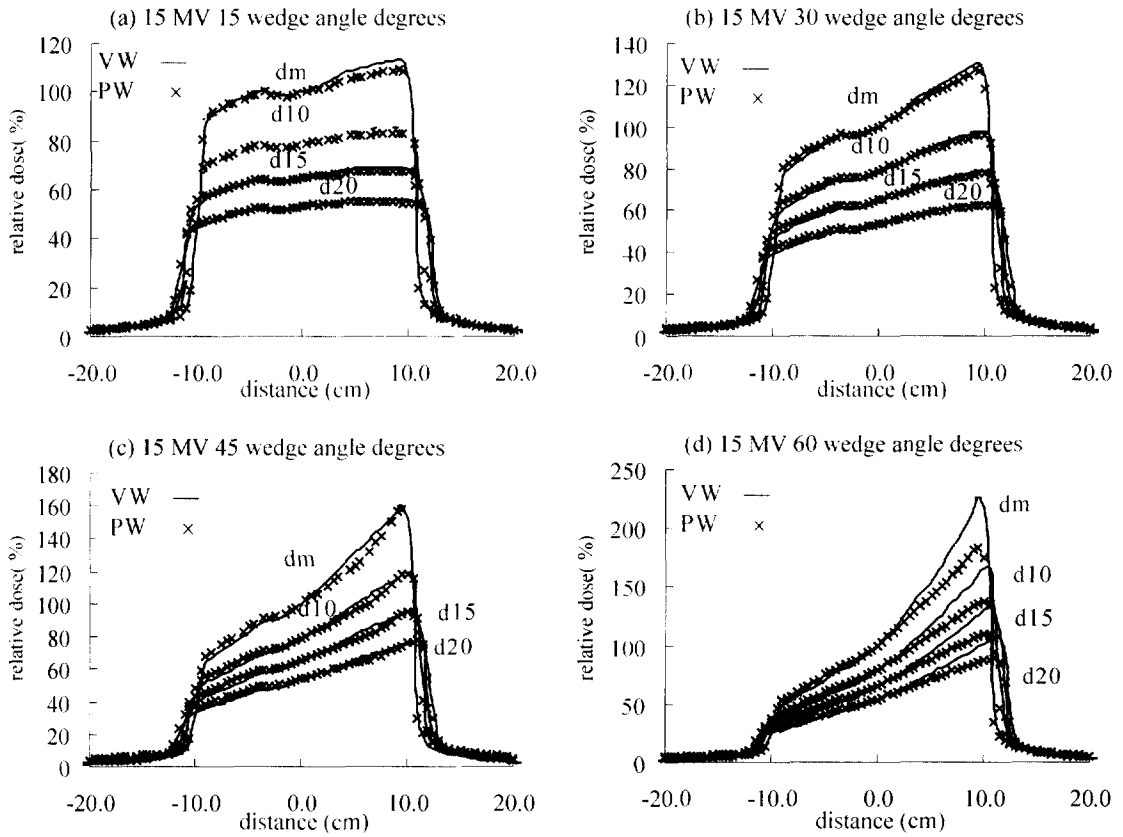

Figure 4. Profiles of the 15 MV 20×20 cm² field with physical wedges ("PW") and virtual wedges ("VW") at depths of d_{max} ("dm"), 10 cm ("d10"), 15 cm ("d15"), and 20 cm ("d20"). Dose is normalized to 100% at the d_{max} along the central axis.

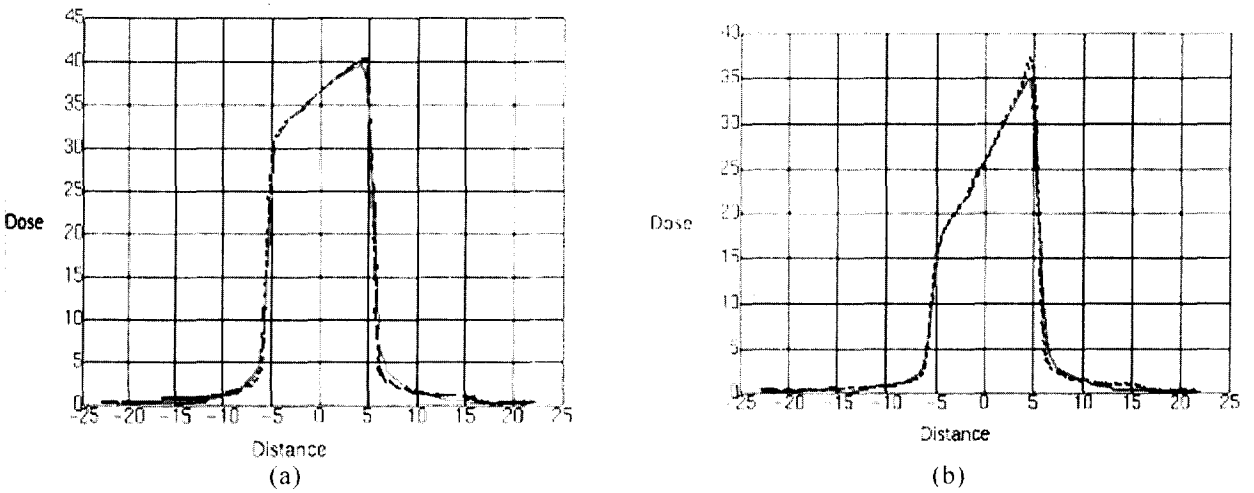

Figure 5. Central-axis measured (solid line) and calculated dose (dotted line) profiles at depth of 5 cm for 6 MV. (a) 10×10 cm² field with 30° virtual wedge. (b) 10×10 cm² field with 60° virtual wedge.

Treatment planning

The percentage difference between the calculated and measured wedged dose distribution data was determined as: (calculated-measured)/measure d_{max} × 100%. Excluding large wedge angles and large field sizes calculations in the toe side of VW, agreement between calculations and measurements was within 2%. Figure 5 depicts the comparison of isodose profiles for VW between the calculations and measurements.

Figure 6 illustrates the actual treatment plan. When the same beam orientations and relative weightings were used for both plans, hot spot increased with VW for 30° wedged fields. In order to reduce the hot spot, 40° VW fields were used. Another clinical case of prostate cancer was demonstrated in Figure 7. Figure 7(a) presents our routine treatment plan for segmental open fields. There were six beam fields, including 45°, 90°, 135°, 225°, 270°, and 315° gantry angles. Figure 7(b) presents the previous fields with VW and the same weightings. In terms of homogenous dose coverage (see the 95% isodose of Figure 7(b)), the VW plan produced better results.

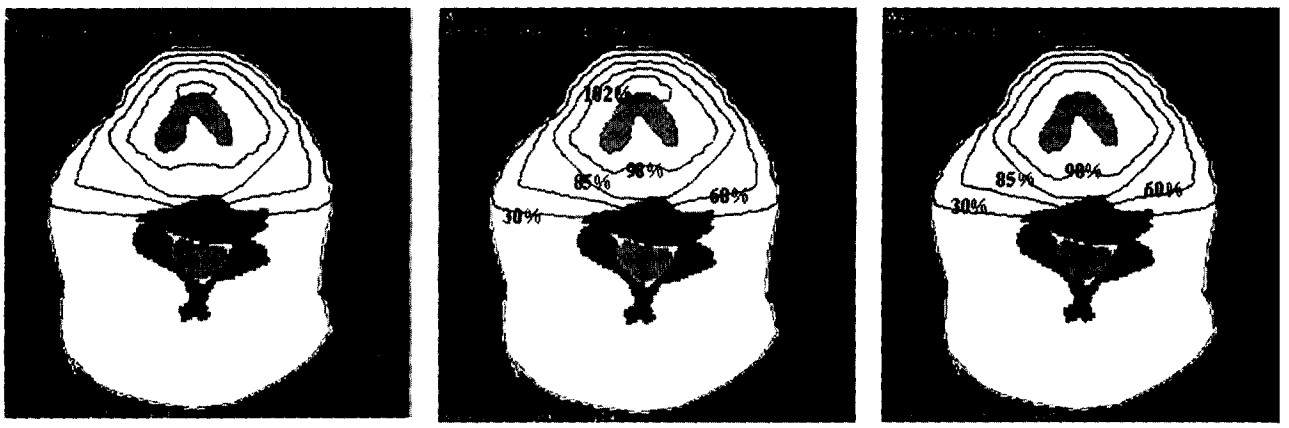

(a) (b) (C)

Figure 6. Comparison of treatments plans for a larynx treatment with 6 MV. (a) Isodoses for the 30° physical wedges, (b) isodoses for the 30° virtual wedges, and (c) isodoses for the 40° virtual wedges.

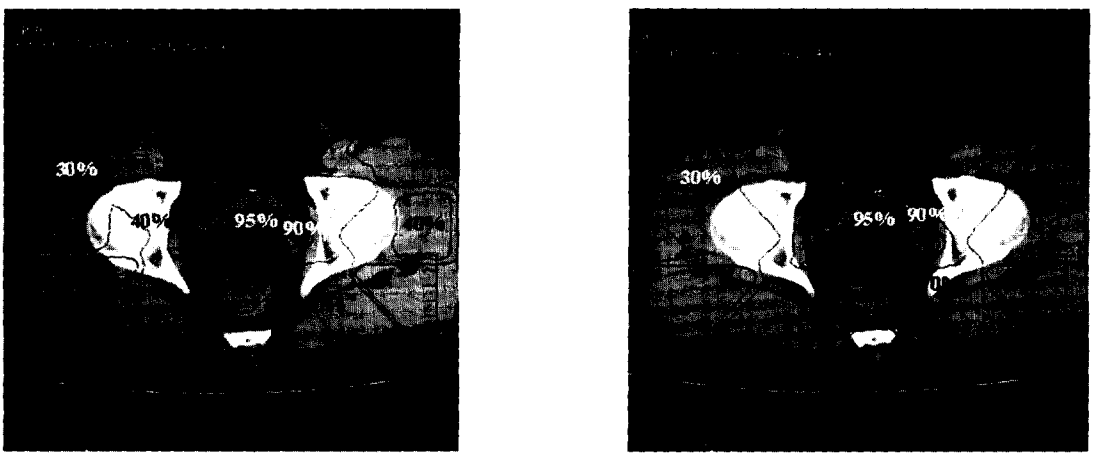

(a) (b)

Figure 7. Comparison of treatment plans for prostate cancer with 6 MV. (a) Isodoses for the open field. (b) Isodoses for the 20° virtual wedges.

Discussion and Conclusion

One of the advantages of VW is that the WFs are unit and the error is within 1%. In contrast, WFs depend on field size characterizes dynamic and enhanced dynamic wedges. Klein et al. [3] ascertained a nonlinear relationship between WF and field size. However, the PDDs of DW or VW were determined as being closer to those of an open field.

The VW peripheral dose is the dose delivered to tissue outside the collimated radiotherapy beam. In the region beyond the geometric edge of the field, the VW peripheral doses and open field doses were nearly identical when an identical dose was delivered to the central axis. In contrast, the PDD was nearly twice as high when the standard PW was applied. For certain clinical sites (such as contralateral breast), the PDD that a radiotherapy beam generates may be significant. Notably, scatter from a wedge filter can increase the PDD more than that received from an open field for the same given dose. McParland et al. [9] and Warlick et al. [10] reported that the contralateral breast dose that increased by a dynamic or enhance dynamic wedge was only half of that for a PW within an identical situation. Chang *et al.* [11] also reported the same experimental result.

The experimental results of VWs dose profiles indicated that the CA24 chamber array detector was an effective dosimetry system. Since the dose at each measurement point must be obtained via integration during the entire process, it measured dose profiles accurately, and more efficiently than a single chamber does. Therefore, initial chamber array may be a good choice for commissioning of a VW.

However, some authors have employed other measurement systems. For example, a diode array was employed to measure nonphysical wedge profiles [12-14]. However, the dosimetric characteristics of the diode detector depended heavily on processing conditions, including diode type, doping level, device processing technique and pre-irradiation. Therefore, each type of diode array must be evaluated individually prior to measurement.

In addition, film is also a good method to measure dose profiles [3]. It is less time-consuming and has a high spatial density of data. However, it also requires careful measurement of the optical density-to-dose conversion curve at all depths. Film may be used more efficiently for verification purposes, particularly for periodical quality assurance (QA) of the VW.

VW was faster than PW in practical treatment procedures. Van Santvoort [5] studied the beam on time for VW and PW and determined that, with similar cases, VW required less time than PW. A more significant time gain can be expected for VW because the PWs require changing. It is no longer necessary to enter the treatment room between fields; it also promotes a more effective use of remote procedures.

In contrast to PWs, VWs are limited to the Y-direction as only the Y-jaws move dynamically, thus requiring collimator rotation to allow wedge movement in any other direction. Compared with VW, Cerrobend block offers more conformal shielding than the Siemens that has 1 cm leaves. In some cases, the wedge direction that is perpendicular to the leaf direction might be inconvenient. Therefore, a block would be used if necessary.

Prior to activating the beam, the jaw that creates the VW is moved to the opposing jaw. Subsequently the field is closed to 1 cm (projected at source to axis distance (SAD)). This 1 cm gap creates a somewhat sharper edge at the toe of the wedge field. Irradiation begins with the gap, thus megavoltage imaging cannot be performed using the treatment field. Therefore, an electronic portal imaging device (EPID) cannot be used for clinical imaging in treatments that use VW [3]. The other disadvantage of a gap (>1 cm) is that with large field sizes, a plateau region of dose appears in the gap area and along the toe side of VW occurs [15].

Any arbitrary wedge angle (typically 15-60 degrees) can be created for VW instead of the traditional four fixed wedges (typically 15, 30, 45, and 60 degrees) for PW. However, due to limited time and practice, only a limited number of wedge angles were selected for our study. In our experiment, seven types of wedge angles, those typical fixed wedge angles and an additional 20, 40, and 50 degrees, respectively, were used.

Delivery of a wedge beam requires accurate functioning of several components of the linear accelerator hardware and software. Therefore, VW QA programs are essential. Rathee et al. [16] presented several QA programs for VW and their experimental results indicate that wedge profiles are very stable over time.

The implementation of VW is an important step towards virtual conformal therapy. Without requiring a heavy metal filter, it creates a wedged-shape isodose distribution by moving one of the asymmetric jaws across the field during treatment. This has produced significant practical and dosimetric improvements. Furthermore, the VW is a reliable tool that can be employed clinically, providing it can be managed through the treatment planning system. Furthermore, it provides superior flexibility and results in shorter activation periods.

References

1. Kijewski PK, Chin LM, Bjarngard BE: Wedge-shaped dose distributions by computer-controlled collimator motion. Med Phys 1978;5:426-9.
2. Leavitt DD, Martin M, Moeller JH, Lee WL: Dynamic wedge field techniques through computer-controlled collimator motion and dose delivery. Med Phys 1990;17:87-91.
3. Klein EE, Low DA, Meigooni AS, Purdy JA: Dosimetry and clinical implementation of dynamic wedge. Int J Radiat Oncol 1995;31:583-92.
4. Yao J: Virtual wedge dose calculation and its impact on radiation treatment planning systems. Med Phys 1995;22:975.
5. van Santvoort J: Dosimetric evaluation of the Siemens Virtual Wedge. Phys Med Biol 1998;43: 2651-63.
6. Liu HH, Lief EP, McCullough EC: Measuring dose distributions for enhanced dynamic wedges using a multichamber detector array. Med Phys 1997;24:1515-9.
7. Niroomand-Rad A, Haleem M, Rodgers J, Obcemea C: Wedge factor dependence on depth and field size for various beam energies using symmetric and half-collimated asymmetric jaw settings. Med Phys 1992;19:1445-50.
8. McParland BJ: Peripheral doses of two linear accelerators employing universal wedges. Brit J Radiol 1990;63:295-8.
9. McParland BJ: The effect of a dynamic wedge in the medial tangential field upon the contralateral breast dose. Int J Radiat Oncol 1990;19:1515-20.
10. Warlick WB, O'Rear JH, Earley L, Moeller JH, Gaffney DK, Leavitt DD: Dose to the contralateral breast: a comparison of two techniques using the enhanced dynamic wedge versus a standard wedge. Med Dosimetry 1997;22:185-91.
11. Chang SX, Deschesne KM, Cullip TJ, Parker SA, Earnhart J: A comparison of different intensity modulation treatment techniques for tangential breast irradiation. Int J Radiat Oncol 1999;45: 1305-14.
12. Leavitt DD, Larsson L: Evaluation of a diode detector array for measurement of dynamic wedge dose distributions. Med Phys 1993;20:381-2.
13. Zhu TC, Ding L, Liu CR, Palta JR, Simon WE, Shi J: Performance evaluation of a diode array for enhanced dynamic wedge dosimetry. Med Phys 1997;24:1173-80.
14. Verhaegen F, Das IJ: Monte Carlo modelling of a virtual wedge. Phys Med Biol 1999;44:251-9.
15. Miften M, Zhu XR, Takahashi K, Lopez F, Gillin MT: Implementation and verification of virtual wedge in a three-dimensional radiotherapy planning system. Med Phys 2000;27:1635-43.
16. Rathee S, Kwok CB, MacGillivray C, Mirzaei M: Commissioning, clinical implementation and quality assurance of Siemen's Virtual Wedge. Med Dosim 1999;24:145-53.

動態虛擬式楔形濾器之劑量分佈探討

林招膨[1,2,3] 張東浩[1,4] 王愛義[2] 劉幕台[1,2,3,5] 陳苑蓉[1,4] 郭瓊文[2] 賴源淳[1]

背景與目的：本研究針對動態虛擬式楔形濾器的臨床特性，包括動態虛擬式楔形濾器角度驗證，楔形濾器穿透因子，百分深度劑量，與劑量分佈剖視圖各項做探討。

方法：使用 Wellhöfer IC15 游離腔與 CU500E 6177 電子劑量計於 48×48×40 cm^3 水假體中量測角度，穿透因子，百分深度劑量等各項因子。並利用 CA24 陣列式游離腔，量測劑量分析剖視圖。動態式楔形濾器以直線加速器機頭控制上準直儀等速度移動及劑量率的變化，達成所想要的實體楔形濾器角度的劑量分佈剖視圖。動態虛擬式楔形濾器劑量分佈物理特性包括了在不同深度與照野下虛擬角度的驗證，實體與動態虛擬式楔形濾器百分深度劑量與楔形濾器穿透因子及剖視圖的區別。

結果：動態虛擬式楔形濾器設定角度與機器實際角度誤差 1°內。所有動態虛擬式楔形濾器穿透因子均近於 1.0，誤差在 1%以內。而 60°楔形濾器其照野在 20×20 到 24×24 cm^2，其誤差約爲 2-3%。動態虛擬式楔形濾器之百分深度劑量較接近開放照野之百分深度劑量。

結論：不管是臨床上或劑量學上，動態虛擬式楔形濾器在放射治療計畫中均較實體楔形濾器更具實用性。在臨床實務的應用上，更方便作爲治療的設定，可有更多角度的選擇性。本文具體討論了這些臨床劑量分佈的特性及其臨床應用。隨之，動態虛擬式楔形濾器每日每月的品質保證課程更增進了其在治療計畫中的品質。（彰化醫學 2003;**8**:87-97）

關鍵詞：動態虛擬式楔形濾器，楔形濾器穿透因子，動態虛擬式楔形濾器角度

[1]台灣彰化，彰化基督教醫院放射腫瘤科；[2]台灣新竹，元培科學技術學院放射技術系；[3]台灣台北，國立台灣大學醫學院附設醫院腫瘤醫學部；[4]台灣新竹，國立清華大學原子科學系；[5]台灣台中，中山醫學大學醫學系

受文日期：91 年 9 月 23 日，修改日期：92 年 1 月 14 日，接受刊登：92 年 2 月 18 日

索取抽印本請聯絡：張東浩醫師，台灣，彰化市 500 南校街 135 號，彰化基督教醫院，放射腫瘤科。